Chen *et al. Microbial Cell Factories* (2024) 23:237
https://doi.org/10.1186/s12934-024-02515-w

Microbial Cell Factories

RESEARCH Open Access

Elucidating the salt-tolerant mechanism of *Halomonas cupida* J9 and unsterile ectoine production from lignocellulosic biomass

Yaping Chen[1], Yujie Liu[1], Yan Meng[1], Yuting Jiang[1], Weini Xiong[1], Shufang Wang[2*], Chao Yang[1*] and Ruihua Liu[3*]

Abstract

Background Ectoine as an amino acid derivative is widely applied in many fields, such as the food industry, cosmetic manufacturing, biologics, and therapeutic agent. Large-scale production of ectoine is mainly restricted by the cost of fermentation substrates (e.g., carbon sources) and sterilization.

Results In this study, *Halomonas cupida* J9 was shown to be capable of synthesizing ectoine using xylose as the sole carbon source. A pathway was proposed in *H. cupida* J9 that synergistically utilizes both WBG xylose metabolism and EMP glucose metabolism for the synthesis of ectoine. Transcriptome analysis indicated that expression of ectoine biosynthesis module was enhanced under salt stress. Ectoine production by *H. cupida* J9 was enhanced by improving the expression of ectoine biosynthesis module, increasing the intracellular supply of the precursor oxaloacetate, and utilizing urea as the nitrogen source. The constructed J9U-P8EC achieved a record ectoine production of 4.12 g/L after 60 h of xylose fermentation. Finally, unsterile production of ectoine by J9U-P8EC from either a glucose-xylose mixture or corn straw hydrolysate was demonstrated, with an output of 8.55 g/L and 1.30 g/L of ectoine, respectively.

Conclusions This study created a promising *H. cupida* J9-based cell factory for low-cost production of ectoine. Our results highlight the potential of J9U-P8EC to utilize lignocellulose-rich agriculture waste for open production of ectoine.

Keywords Salt-tolerant mechanism, Lignocellulosic biomass, Unsterile ectoine production, Promoter engineering, *Halomonas cupida*

Introduction

Ectoine, a compatible solute accumulated by halophilic microorganisms, plays important roles in improving cellular resistance to high temperature, radiation, drought, and high osmotic pressure [1, 2]. Ectoine is widely used as functional components in food, cosmetic and biologics, and it has an annual demand of approximately 15,000 tons and a market price of ~$1,000/kg [1–3].

In recent years, microbial production of ectoine has emerged as a promising alternative to traditional chemical synthesis, offering an economically

*Correspondence:
Shufang Wang
wangshufang@nankai.edu.cn
Chao Yang
yangc20119@nankai.edu.cn
Ruihua Liu
yangyangliu@nankai.edu.cn
[1]Key Laboratory of Molecular Microbiology and Technology for Ministry of Education, College of Life Sciences, Nankai University, Tianjin 300071, China
[2]Key Laboratory of Bioactive Materials for Ministry of Education, College of Life Sciences, Nankai University, Tianjin 300071, China
[3]Tianjin Key Laboratory of Protein Science, College of Life Sciences, Nankai University, Tianjin 300071, China

feasible and environmental friendly approach to large-scale production [2]. The ectoine biosynthetic pathways have been intensively researched in halophilic microorganisms [4, 5]. Two major strategies of ectoine biosynthesis are proposed, including the production of ectoine by halophilic bacteria and heterologous production of ectoine by *Escherichia coli* and *Corynebacterium glutamicum* [6–11]. Moreover, two genome-editing approaches have been developed in halophilic bacteria, including CRISPR/Cas9 and suicide plasmid/counterselection [12–14]. Unsterile production of high value-added products such as polyhydroxyalkanoate (PHA) and ectoine by halophilic bacteria-based cell factories has been achieved by utilizing anti-microbial contamination of halophilic bacteria [9, 15], which highlights the potential of halophilic bacteria as chassis cells for the next-generation industrial biotechnology (NGIB) [16]. In previous studies, engineered *Halomonas hydrothermalis* Y2 and *H. bluephagenesis* TD01 could produce 3.13 and 6.3 g/L ectoine in shake-flask fermentation using glucose as the carbon source, respectively [8, 9]. Since the vast majority of ectoine producers utilize cereal crops derived carbohydrates as the carbon sources, the large-scale production of ectoine is restricted by high substrate cost and limited cereal resource.

Currently, the biosynthesis of bioplastics, biofuels and platform chemicals by using sustainable and cost-effective carbon sources such as lignocellulose and methane has become a research hotspot [17–22]. Lignocellulosic biomass (LCB) with abundant and stable sources has a global annual production of more than 1.5 trillion tons [23, 24]. Glucose and xylose are two main monosaccharides derived from the enzymatic hydrolysis of cellulose and hemicellulose components of lignocellulose [22]. Most ectoine-producing strains are unable to utilize xylose, thus, high-value bioconversion of xylose has become a critical challenge in the production of ectoine from LCB. Tanimura et al. [17] constructed the △*ectD* mutant strain of *H. elongata*, with the ectoine yield of 53.53 mg/g fresh cell weight using glucose and xylose as the co-carbon sources. Recently, *Methylotuvimicrobium alcaliphilum* 20Z was metabolically engineered to simultaneously utilize methane, glucose and xylose to produce ectoine by introducing glucose and xylose metabolism modules from *E. coli* and *Zymmonas mobilis*, and the finally constructed strain 20ZXG/Δ*ectR1* grown on methane, glucose and xylose reached the ectoine yield of 37.93 ± 3.27 mg/g dry cell weight [22].

In this study, a halophilic bacterium *H. cupida* J9, which was previously isolated by our lab from high-salt wastewater [25], was demonstrated to be capable of producing ectoine from either glucose or xylose. Moreover, the salt-tolerant mechanism of *H. cupida* J9 was elucidated by genome and transcriptome analysis. Furthermore, the engineered bacterium J9U-P8EC was constructed by inserting the strong promoter P8 in the upstream of the *ectABC* and *ppc* genes, which resulted in an increased production of ectoine from either xylose or a glucose-xylose mixture. Finally, the capacity of J9U-P8EC to utilize corn straw hydrolysate for ectoine production was confirmed in an open fermentation process.

Materials and methods

Strains and culture conditions

E. coli strains were cultivated in Luria-Bertani (LB) medium [26] at 37 °C. *H. cupida* J9U (J9 △*upp*) and its mutants were cultured in high-salt LB medium containing extra 50, 90 and 150 g/L NaCl (LB60, LB100 and LB150) and mineral salt medium [22] supplemented with 30 g/L glucose (MMG) at 37 °C. The salt concentration of the fermentation medium was 60 g/L, which is the optimal for the growth of *H. cupida* J9. Mineral salt medium plus 3 g/L urea (MM3) was used as the optimized medium. For ectoine production, *H. cupida* strains were used in MM3 supplemented with 30 g/L glucose (MMG3), MM3 supplemented with 30 g/L xylose (MMX3), and MM3 supplemented with 20 g/L xylose and 10 g/L glucose (MMXG3) at 37 °C and 200 rpm for 60 h. The preparation of lignocellulose hydrolysate medium MML3 is described in Sect. 2.5. When required, the media were supplemented with 50–100 μg/mL kanamycin (Kan) or 100 μg/mL 5-fluorouracil (5-FU).

RNA-seq and RT-qPCR analysis

After J9U was cultivated in LB60, LB100 and LB150 at 37 °C and 200 rpm for 12 h, 5 mL of the culture broths were centrifuged to collect the mid-log phase cells. Total RNA samples were extracted from the cells and purified according to previous protocols [27]. Quality control of RNA samples was performed by electrophoresis on an Agilent 2100 Bioanalyser. RNA samples with high purity and integrity were used to construct sequencing library. Libraries were sequenced on an Illumina Novaseq 6000 by Shanghai Majorbio Biopharm Technology Co., Ltd. Differentially expressed genes (DEGs) in J9U cells grown in media containing different salt concentrations were determined using the DESeq2 package. Statistical enrichment of gene ontology (GO) was performed using Goatools (https://github.com/tanghaibao/GOatools) and Fisher's exact test.

mRNA extracted from J9U cells was reverse transcribed to cDNA using a HiScript II Q RT SuperMix (Vazyme). Real-time qPCR was performed using

cDNA and a ChamQ Universal SYBR qPCR Master Mix (Vazyme) on a real-time qPCR system (Applied Biosystems). The $2^{-\Delta\Delta Ct}$ method [28] was used to calculate the relative transcription levels of the *ppc*, *lysC*, *asd*, *ectA*, *ectB*, *ectC*, *ectD* and *doeA* genes in J9U using the 16 S rRNA gene as the internal reference. Primers for RT-qPCR are listed in Table S1.

Construction of H. Cupida mutants

In this study, a genome-editing approach based on suicide plasmid/counterselection described in Wang et al. [14] was used to construct *H. cupida* mutants. Firstly, the P8 promoter from *Pseudomonas putida* KT2440 ($P8_{KT}$) [29] plus ribosome binding site was spliced with two homologous arms by overlap PCR [30], and the fusion fragment was ligated into the *upp*-containing pKJU (derived from a suicide plasmid pK18mobsacB [31], to generate pKJU-P8-ectABC and pKJU-P8-ppc. Subsequently, the promoter knock-in vectors were introduced into a 5-FU resistant mutant J9U (J9 Δ*upp*) [14] by conjugative transfer using *E. coli* S17-1 as the donor strain. The *upp* gene encodes uracil phosphoribosyltransferase, which catalyzes the conversion of 5-fluorouracil (5-Fu) to 5-fluorodeoxyuracil monophosphate, thereby inhibiting cell growth. The single- and double-crossover mutants were screened by the Kan and 5-FU resistance on LB60 agar plates supplemented with 100 μg/mL Kan and 5-FU, respectively, to obtain the promoter knock-in mutants J9U-P8E and J9U-P8EC. To obtain the *ectABC* knockout mutant J9U-dE, the construction of *ectABC* knockout vector, the introduction of knockout vectors into J9U, and the screening of the single- and double-crossover mutants were performed as described in the construction of promoter knock-in mutants. Finally, the successful construction of J9U-dE, J9U-P8E and J9U-P8EC was confirmed by DNA sequencing. The strains, plasmids, and primers used for mutant construction are listed in Table 1 and S1.

Shake-flask fermentation for ectoine production

A single colony of J9U and its mutants were cultivated overnight in a tube containing 5 mL of LB60 at 37 °C and 200 rpm. Then, the primary seed culture was transferred to a 500 mL flask containing 100 mL of LB60 at a 1% (v/v) ratio and cultured at 37 °C and 200 rpm for 12 h. Subsequently, the secondary seed culture was inoculated into a 500 mL flask containing 100 mL of ectoine fermentation media (MMG3, MMX3 and MMXG3) (Sect. 2.1.) at a 5% (v/v) ratio and fermented at 37 °C and 200 rpm for 60 h. For ectoine extraction, the fermentation broth (1 mL) was transferred to a 1.5 mL freezing tube with 95% zirconia beads, and then the cells were thoroughly lysed by centrifugation at 2,400 *g* for 90 s using a high-efficiency tissue cell-destroyer 1000 (Xinzongke Biotech Co. Ltd.). Next, the mixture was transferred to a 1.5 mL Eppendorf tube and centrifuged at 4 °C and 13,500 *g* for 10 min. The supernatant was collected and passed through a 0.22 μm organic pore filter. To determine the ectoine content, samples were subjected to LC/MS analysis (Sect. 2.6.). To determine cell dry weight (CDW), the fermentation broth was centrifuged at 4 °C and 13,500 *g* for 10 min to collect the cells, and then the cells were lyophilized in a vacuum freeze dryer for 24 h and weighed. Growth and sugar consumption by J9U-P8EC, J9U-P8E and J9U were measured in ectoine fermentation media using the methods described in Sect. 2.6.

Ectoine production from corn straw hydrolysate

Corn straw powder was dried at 60 °C and pretreated with 2% H_2SO_4 at 100 °C for 2 h in a 10:1 liquid-to-solid ratio. Then, enzymatic hydrolysis of the hydrolysate

Table 1 Strains and plasmids used in this study

Strains and Plasmids	Description	Reference
Strains		
Echerichia coli Trans1-T1	F^- φ80 (*lacZ*) ΔM15 Δ*lacX* 74*hsdR* (r_k^-, m_k^+) Δ*recA*1398 *endA*1 *tonA*	This lab
Echerichia coli S17-1 pir	RP4-2 (Km::Tn7,Tc::Mu-1), *pro-82*, *LAMpir*, *recA1*, *endA1*, *thiE1*, *hsdR17*, *creC510*	This lab
Halomonas cupida J9	wild type	This lab
J9U	J9 Δ*upp*	This lab
J9U-dE	J9U derivative with knockout of *ectABC*	This work
J9U-P8E	J9U derivative with integration of the P8 promoter into upstream of *ectABC*	This work
J9U-P8EC	J9U-P8E derivative with integration of the P8 promoter into upstream of *ppc*	This work
Plasmids		
pK18mobsacB	Kan^r, a suicide plasmid for gene knockout or knock-in	This lab
pKJU	Kan^r, pK18mobsacB derivative containing the *upp* gene	This lab
pKJU-dE	Kan^r, a pKJU derivative, used to delete *ectABC*	This work
pKJU-P8-ectABC	Kan^r, a pKJU derivative, used to insert the P8 promoter into upstream of *ectABC*	This work
pKJU-P8-ppc	Kan^r, a pKJU derivative, used to insert the P8 promoter into upstream of *ppc*	This work

was performed with 30 FPU of Cellic CTec3 HS (Novozymes) at 50 °C and pH 5.0 for 36 h (0.5 ml of enzyme for every 100 ml of hydrolysed solution). To adsorb toxic substances (including phenolic compounds, furfural, HMF, and acetic acid) from the non-saccharide compounds [32], 0.5% (w/v) activated carbon (Aladdin) was added to the hydrolysate, and the suspension was then incubated at 50 °C and 150 rpm for 60 min. Finally, the insoluble matter was removed by centrifuging the suspension at 9,800 *g* for 10 min, to obtain the straw hydrolysate with a xylose to glucose ratio of 3:1 and a total sugar concentration of 30 g/L. To use straw hydrolysate as the carbon source for ectoine production, the MML3 medium was prepared by dissolving all components of MM3 in the straw hydrolysate. J9U-P8EC or J9U was inoculated into a 500 mL flask containing 100 mL of MML3 and fermented at 37°C and 200 rpm for 60 h. Growth and sugar consumption by J9U-P8EC and J9U were measured in MML3 using the methods described in Sect. 2.6. The ectoine titre and CDW at the end of fermentation were determined as described in Sect. 2.4. *and 2.6.*

Analytical methods

The ectoine content was determined using Agilent Q-TOF LC/MS equipped with an InfinityLab Poroshell 120 SB-Aq column. Acetonitrile and water (2:98, v/v) was used as the mobile phase at a flow rate of 0.5 mL/min. The column temperature was maintained at 30 °C. The UV detection wavelength was set at 220 nm. Cell density ($OD_{600\ nm}$) of J9U and its mutants grown in media was monitored using a UV-1900i spectrometer (Shimadzu). A SBA-40D biosensor equipped with glucose and xylose oxidase electrodes (Shandong Academy of Sciences) was used to detect the concentration of glucose and xylose in the fermentation broth.

Results and discussion

Elucidating the salt-tolerant mechanism of H. Cupida J9

Halophilic bacteria combat high-salt environments by accumulating compatible solutes and synthesize ectoine as the major low molecular weight compatible solutes [4, 6]. Ectoine biosynthesis pathway is highly conserved among halophilic microorganisms and has been intensively studied [4, 6, 8, 9]. In this study, whole-genome sequencing and functional annotation of *H. cupida* J9 suggests that the complete ectoine biosynthesis pathway is present in the genome of *H. cupida* J9. This pathway mainly consists of aspartate kinase (*lysC*), aspartate semialdehyde dehydrogenase (*asd*), 2,4-diaminobutyryltransferase (*ectA*), 2,4-diaminobutyric acid transferase (*ectB*), and ectoine synthase (*ectC*) (Fig. S1). The sequencing results reveal that single-copy *ectA*, *ectB* and *ectC* genes form the *ectABC* cluster within a shared operon in the genome *H. cupida* J9. The genome sequence of *H. cupida* J9 was deposited in the GenBank database under accession no. ON045848.

To elucidate the role of ectoine in improving salt tolerance of *H. cupida* J9, the mutant lacking *ectABC* (J9U-dE) were constructed. The growth inhibition was observed with *ectABC* knockout mutant under high salt conditions. The growth rate and the final cell density of LB60-grown J9U-dE were lower than that of J9U (Fig. 1A). The *ectABC* knockout mutant J9U-dE lost the capability to synthesize ectoine and the growth of J9U-dE was significantly inhibited by high salt concentrations (Fig. 1B and C), which clearly indicated that the accumulation of ectoine by *H. cupida* J9 played crucial roles in improving salt tolerance of *H. cupida* J9. Production of ectoine by *H. cupida* J9 was verified by LC-MS analysis of fermentation products. The retention time of a chromatographic peak in the HPLC chromatograms of the fermentation products corresponded to that of the authentic standard of ectoine, and the compound corresponding to the peak had the same mass spectrogram compared to the authentic standard of ectoine (Fig. S2). In addition, J9U accumulated 0.26, 0.40 and 0.68 g/L ectoine, respectively, when grown in LB60, LB100 and LB150 (Fig. 1D). Ectoine accumulation by J9U increased with the increase of salt concentration, suggesting that salt stress may stimulate the synthesis of ectoine in J9U.

Correlation of the transcription of ectoine metabolism modules with salt stress

Three transcriptome samples, named H6 (6% NaCl), H10 (10% NaCl) and H15 (15% NaCl), were used to assess the DEGs in J9U under the stimulation of different salt concentrations. As shown by the inter-group difference analysis, 551 DEGs including 192 upregulated and 359 downregulated genes were found by a comparison of H6 and H10. 1126 DEGs including 669 upregulated and 457 downregulated genes were found by a comparison of H10 and H15. 1310 DEGs comprising 700 upregulated and 610 downregulated genes were found by a comparison of H6 and H15 (Fig. S3A). Venn diagram analysis indicated that the numbers of unique genes in three comparative groups were 113, 270 and 355, respectively, with 147 genes being common across three comparative groups (Fig. S3B).

A total of 1341 DEGs were annotated using the GO database. Among them, 692, 547 and 102 DEGs were associated with molecular function, cellular component and biological process, respectively (Fig. 2A). Under salt stress, nearly all genes related to ectoine synthesis displayed an upregulation trend, notably

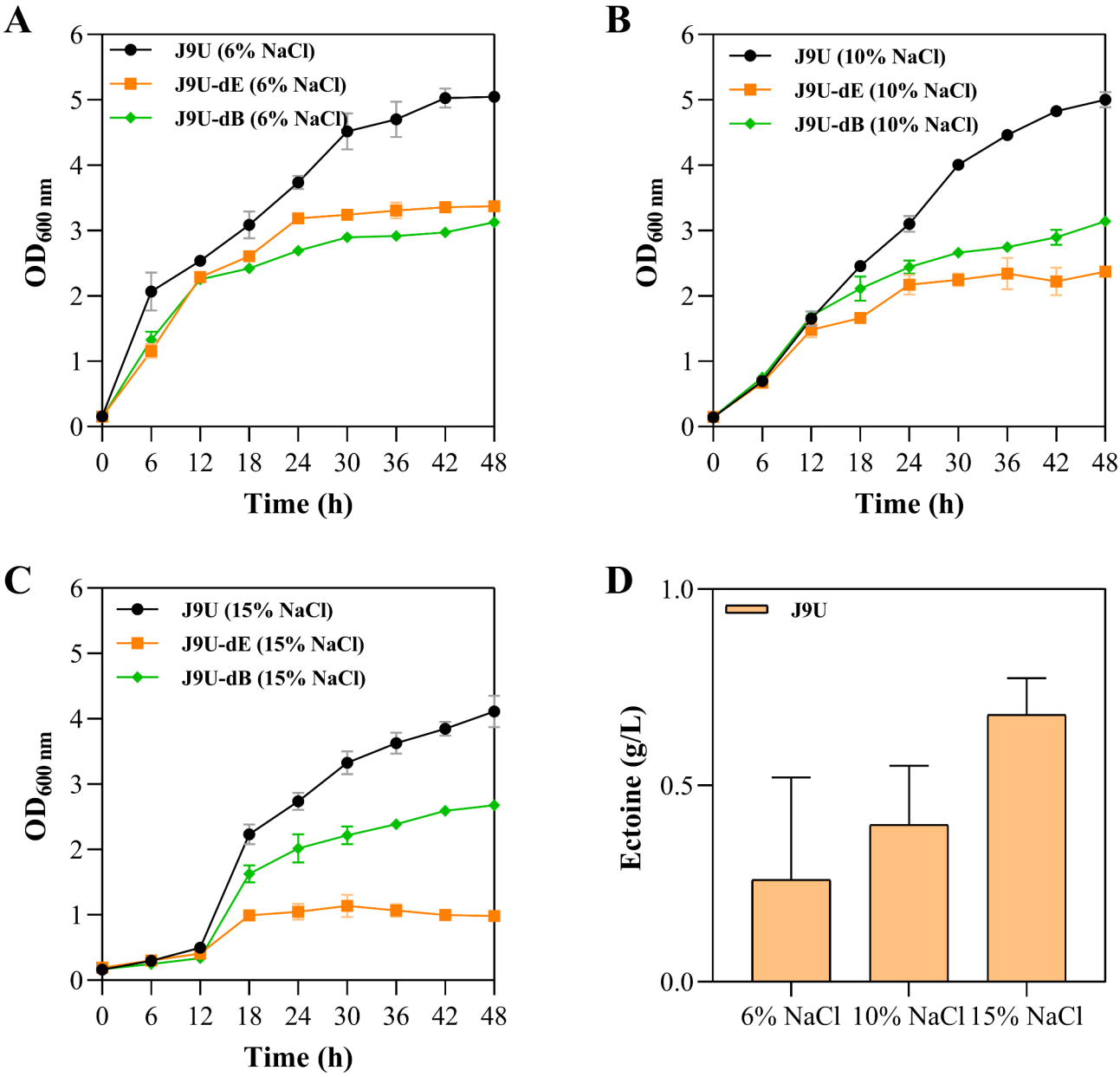

Fig. 1 (**A**, **B** and **C**) Growth curves of J9U, J9U-dE and J9U-dB (**D**) Ectoine accumulation by J9U under salt stress. These strains were cultured at 37 °C and 200 rpm in LB60, LB100 and LB150. The data represent the mean ± standard deviation of triplicate measurements

with significantly elevated transcription levels of the *ectB*, *ectC* and *ectD* genes. Within the PPO-node, the transcription levels of *ppc* (encoding phosphoenolpyruvate carboxylase) and *pyk* (encoding pyruvate kinase) genes were also elevated. Additionally, those genes associated with ectoine metabolism displayed varying degrees of upregulation (*doeA*, *doeB* and *hom*) or downregulation (*doeC* and *doeD*) (Fig. 2B). Furthermore, the DEGs associated with ectoine synthesis under salt stress were validated by RT-qPCR. We found that the transcription levels of ectoine synthesis related genes (*ectB*, *ectC* and *ectD*) were gradually elevated with increasing salt concentration (Fig. 2C). Overall, the transcription of ectoine metabolism modules is more active in *H. cupida* J9 under salt stress.

Genome analysis reveals the pathway for the biosynthesis of ectoine from xylose

In this study, we have identified enzymes involved in the Weimberg pathway (WBG pathway) for xylose utilization in the J9U genome, including xylose dehydrogenase (*xylB*), xylose dehydratase (*xylD*), and 2,5-diketo-D-gluconic acid reductase (*aldH*). This

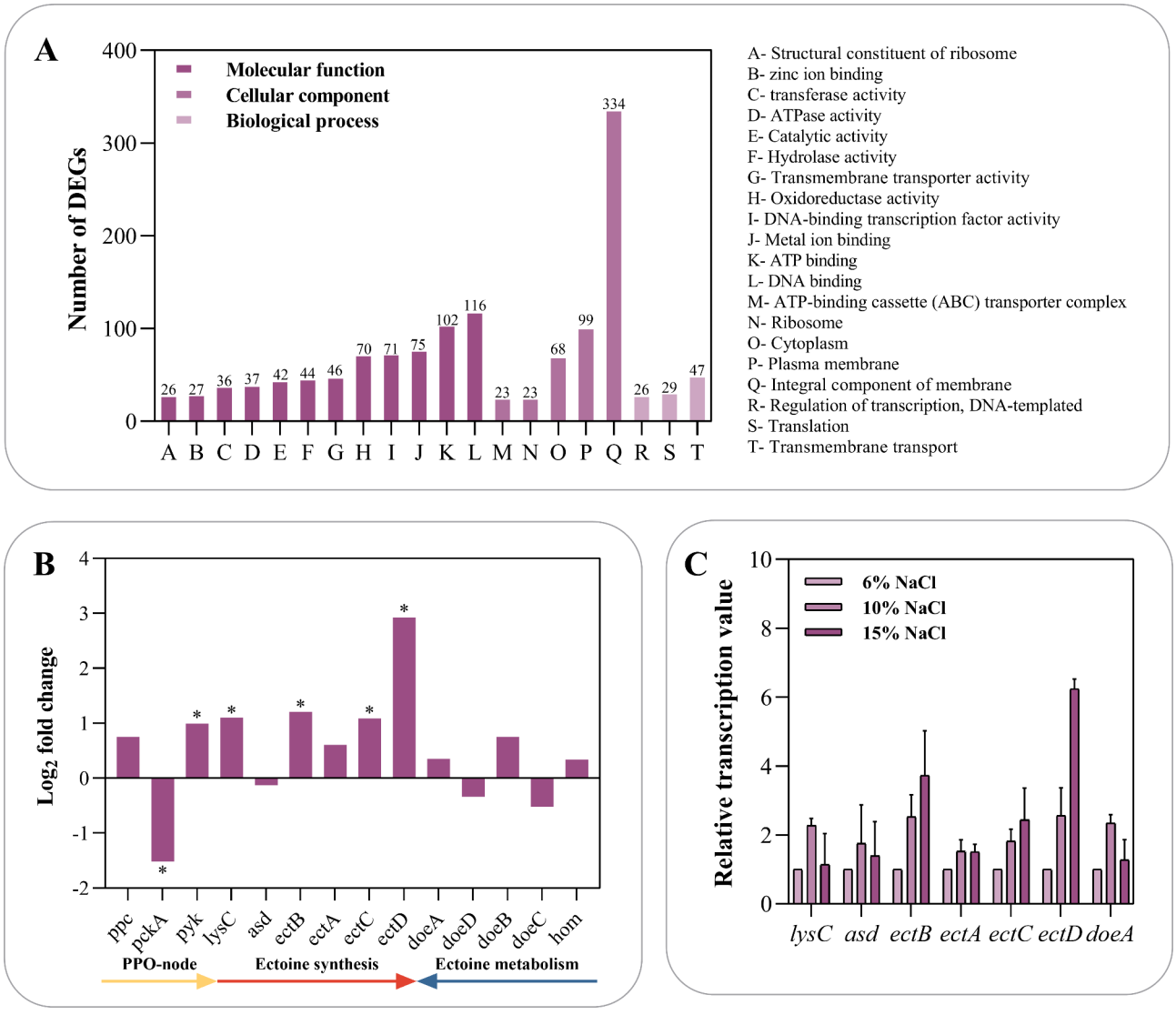

Fig. 2 Transcriptome analysis of *H. cupida* J9 and RT-qPCR analysis of ectoine synthesis related genes under salt stress. (**A**) GO annotation of differentially expressed genes in comparative transcriptome analysis of three samples under salt stress. (**B**) Inter-group differential expression levels of ectoine synthesis related genes as shown by comparative transcriptome analysis of three samples under salt stress. (**C**) RT-qPCR assays for measuring the transcription levels of ectoine synthesis related genes under salt stress. The transcription levels of the endogenous genes in LB60 were set as 1. Detailed procedures for RNA-seq and RT-qPCR analysis are described in Sect. 2.2

pathway operates without carbon loss and feeds directly into the central metabolism's TCA cycle via the end product 2-oxoglutarate. Based on this, a pathway for ectoine biosynthesis from xylose in *H. cupida* J9 was proposed (Fig. 3), which proceeds through xylonate, 2-dehydro-3-deoxy-D-xylonate, 2,5-dioxopentanoate, 2-oxoglutarate, oxaloacetate, aspartate, and L-aspartate-β-semialdehyde, and eventually enters the ectoine biosynthesis module [4, 5]. Fermentation results demonstrated that MMX3-grown *H. cupida* J9 efficiently utilized xylose as the sole carbon source to synthesize ectoine (Fig. S7).

Furthermore, the J9U genome contains both the WBG xylose metabolism pathway and the EMP glucose metabolism pathway (Fig. 3), indicating its capacity to utilize mixed carbon sources for ectoine synthesis. Fermentation results in Sect. 3.5 and 3.6 indicated that both J9U exhibited highly efficient mixed sugar metabolism, making it optimal halophilic platform for developing engineered strains capable of co-utilizing xylose and glucose (Fig. 4).

Optimization of ectoine fermentation media

The majority of ectoine synthesized by J9U is secreted extracellularly (Fig. S4A). Since a substantial nitrogen supply is required for the efficient production of ectoine by microbes, it is necessary to add additional nitrogen sources to optimize the *C/N* ratio in

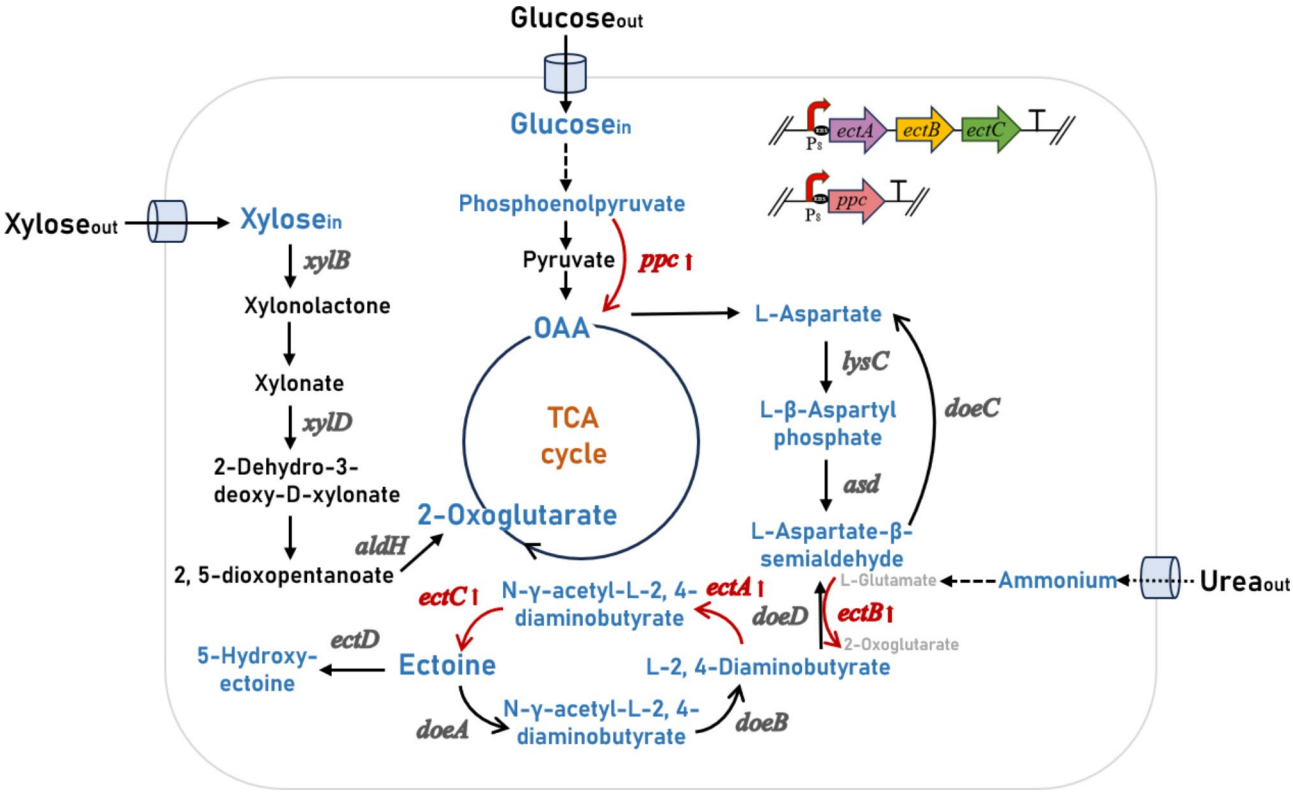

Fig. 3 Proposed pathway for the production of ectoine from xylose and glucose in *H. cupida* J9 and enhanced production of ectoine by overexpressing the *ectABC* and *ppc* genes in *H. cupida* J9. Enzymes: *xylB*, xylose dehydrogenase; *xylD*, xylose dehydratase; *aldH*, 2,5-dioxopentanoate dehydrogenase; *ppc*, phosphoenolpyruvate carboxylase; *lysC*, aspartate kinase; *asd*, aspartate semialdehyde dehydrogenase; *ectB*, 2,4-diaminobutyric acid transferase; *ectA*, 2,4-diaminobutyryltransferase; *ectC*, ectoine synthase; *ectD*, ectoine hydroxylase; *doeA*, ectoine hydrolase; *doeB*, N_2-acetyl-L-2,4-diaminobutanoate deacetylase; *doeC*, aspartate-semialdehyde dehydrogenase; *doeD*, L-2,4-diaminobutyrate transaminase

fermentation media [16, 33]. The inorganic nitrogen source $(NH_4)_2SO_4$ in MMG has a low nitrogen content (21%) and lowers the medium pH by the formation of acidic substances, which is unfavorable to the growth of *H. cupida* strains. In contrast, urea with higher nitrogen content (46%) is an efficient organic nitrogen source that can be rapidly utilized by microorganisms [34]. In contrast to $(NH_4)_2SO_4$, intracellular urea is metabolized into NH_4^+ and the weak acid ions CO_3^{2-}, the latter of which results in a gradual decrease in the pH of the surrounding environment [35].

J9U-P8E was used in MMG supplemented with 1, 3, 5, 7–9 g/L urea. Fermentation with MMG plus 5 g/L urea obtained the highest ectoine titre (4.23 g/L), followed by MMG plus 3 g/L urea (Fig. S4B). However, the decrease in the ectoine yield was observed in fermentation with MMG plus 7–9 g/L urea. Considering the ectoine titre and the substrate cost, 3 g/L urea was added as the nitrogen source to fermentation media.

Furthermore, at the end of fermentation, the final pH of the fermentation broth was measured. We found that the final pH of the fermentation broth decreased less significantly (initial pH was 9.0) as the urea concentration increased (Table S2). The addition of 3 and 5 g/L urea as the nitrogen source maintained an optimal pH range during fermentation, which is favorable for strain growth and ectoine synthesis. The addition of 3 g/L urea as a nitrogen source maintains an optimal pH range (5.56 ~ 7.53) during fermentation, which is favorable to strain growth and ectoine synthesis. The pH of the fermentation broths MMX3, MMXG3, and MML3 with 3 g/L urea remained stable between 6.2 and 7.04, thereby confirming the aforementioned observation (Table S2).

Metabolic pathway engineering enhances ectoine biosynthesis

In previous studies, the overexpression of the *phaC* operon, the *itu* operon, and the *srfA* operon with strong promoters can enhance the biosynthesis of PHA, iturin A, and surfactin in *P. putida* KT2440 and *Bacillus amyloliquefaciens* LL3 [36–38]. In this study, the strong promoter $P8_{KT}$ was inserted into upstream of the *ectABC* cluster to enhance the biosynthetic pathway from L-aspartate-β-semialdehyde to ectoine (Figs. 3 and 5A and C). The resulting mutant J9U-P8E accumulated 4.24 g/L ectoine at 60 h in MMG3, with a 38.56% increase compared to J9U (Fig. 5E).

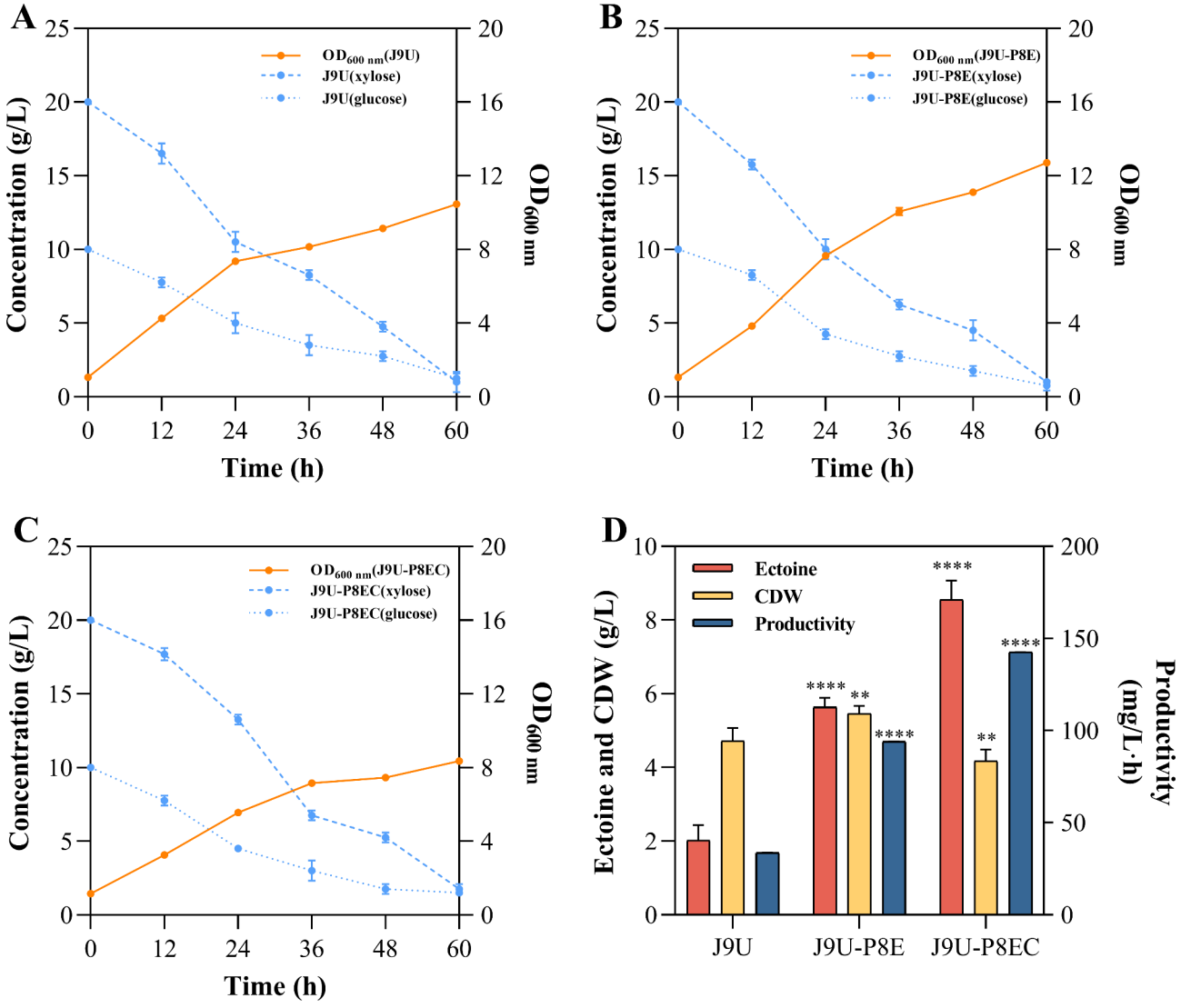

Fig. 4 Cell biomass and ectoine production of MMXG3-grown J9U, J9U-P8E and J9U-P8EC. (**A**, **B** and **C**) Cell growth and total sugar consumption of J9U, J9U-P8E and J9U-P8EC. (**D**) CDW and the titre and productivity of ectoine obtained by fermentation with J9U, J9U-P8E and J9U-P8EC. These strains were cultured in MMXG3 at 37 °C and 200 rpm for 60 h. The data represent the mean ± standard deviation of triplicate measurements. ** and **** indicate $P < 0.01$ and $P < 0.0001$, respectively

Oxaloacetate is a crucial precursor in the biosynthesis of ectoine [4, 11]. In *H. cupida* J9, phosphoenolpyruvate carboxylase (encoded by the *ppc* gene) is responsible for the conversion of phosphoenolpyruvate to oxaloacetate. In this study, the strong promoter $P8_{KT}$ was inserted into upstream of the *ppc* gene in the genome of J9U-P8E, to generate J9U-P8EC (Figs. 3 and 5B and D). When grown in MMG3 for 60 h, J9U-P8EC, J9U-P8E and J9U showed the similar growth trend and glucose consumption trend and the final CDW of the three strains was also similar at 60 h (Fig. S5). The results from RT-qPCR showed that the transcription levels of the *ppc*, *ectA*, *ectB* and *ectC* genes in J9U-P8EC were elevated by 2- to 60-fold compared to those detected in J9U (Fig. S6A). Ectoine accumulation by J9U-P8EC was monitored in a 72 h fermentation period, indicating that the highest ectoine titre was obtained at 60 h (Fig. S6B). J9U-P8EC accumulated 5.06 g/L ectoine at 60 h in MMG3, with a 22.82% increase compared to J9U-P8E (Fig. 5E). In summary, ectoine biosynthesis can be enhanced by enhancing the ectoine biosynthesis module and the intracellular supply of the precursor oxaloacetate in J9U-P8EC.

In previous studies, *P. putida* and *Halomonas* sp. were engineered to metabolize xylose for PHA production [14, 39, 40]. In MMX3 medium, J9U-P8EC achieved an ectoine titre of 4.12 g/L at 60 h (~ 68.67 mg/L·h), a 2.03-fold increase compared to J9U (Fig. 5F). The growth trend and xylose consumption rate of the three strains grown in MMX3 were similar

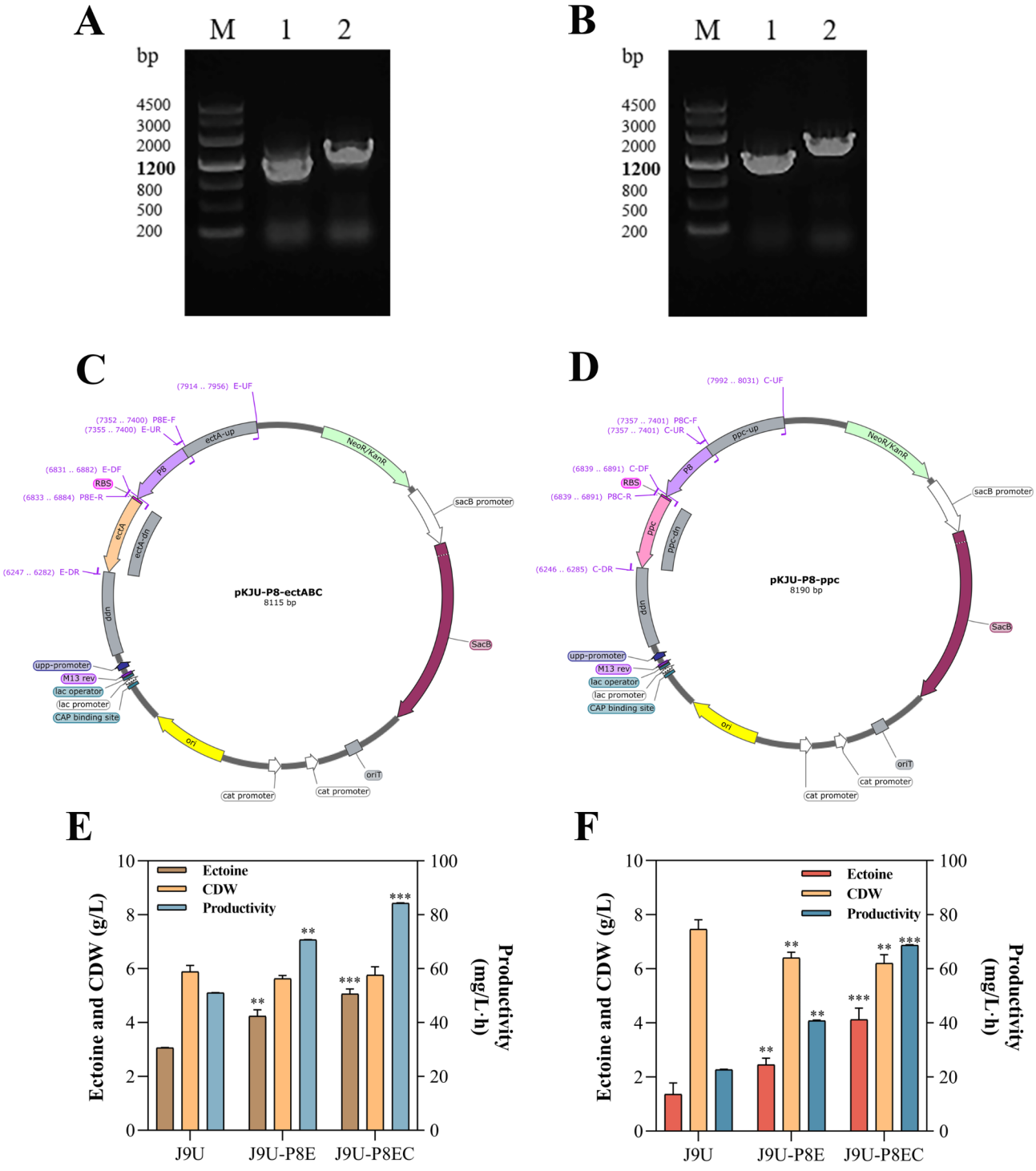

Fig. 5 Colony PCR results, the suicide plasmid maps, and ectoine production of MMG3- and MMX3-grown J9U, J9U-P8E and J9U-P8EC. (**A**) PCR confirmation of the construction of $P8_{KT}$ + RBS insertion mutant J9U-P8E. Lanes: M, Marker Ш; 1, J9U; 2, J9U-P8E. (**B**) PCR confirmation of the construction of $P8_{KT}$ + RBS insertion mutant J9U-P8EC. Lanes: M, Marker Ш; 1, J9U; 2, J9U-P8EC. (**C**) The suicide plasmid map of pKJU-P8-ectABC. (**D**) The suicide plasmid map of pKJU-P8-ppc. All specific PCR primers are listed in Supplementary file 1: Table S1. (**E**) CDW and the titre and productivity of ectoine obtained by fermentation with J9U, J9U-P8E and J9U-P8EC in MMG3 medium. All strains were cultured at 37 °C and 200 rpm for 60 h. (F) CDW and the titre and productivity of ectoine obtained by fermentation with J9U, J9U-P8E and J9U-P8EC in MMX3 medium. All strains were cultured at 37 °C and 200 rpm for 60 h. The data represent the mean ± standard deviation of triplicate measurements. ** and *** indicate $P < 0.01$ and $P < 0.001$, respectively

Table 2 Cell dry weight, ectoine titre, and productivity of three different chassis cells from xylose, glucose and lignocellulosic hydrolysate

Strain	CDW (g/L)	Ectoine (g/L)	Production (mg ectoine/g CDW)	Carbon resource	Reference
J9U	7.46	1.36	182.30	xylose	This work
	4.72	2.02	427.97	xylose, glucose	This work
	4.15	0.51	122.89	lignocellulosic hydrolysate	This work
J9U-P8E	6.4	2.45	382.8	xylose	This work
	5.46	5.64	1032.97	xylose, glucose	This work
J9U-P8EC	6.2	4.12	**664.52**	xylose	This work
	4.17	8.55	**2050.36**	xylose, glucose	This work
	4.25	1.30	**305.88**	lignocellulosic hydrolysate	This work
H. elongata △*ectD*	/	/	49.42 mg/g FW	xylose	[17]
	/	/	53.53 mg/g FW	xylose, glucose	[17]
	/	/	49.84 mg/g FW	lignocellulosic hydrolysate	[22]
M. alcaliphilum 20ZXG/△*ectR*	/	/	37.93	xylose, glucose, methane	[22]

Table 3 The ectoine titre, productivity and conversion efficiency of J9U and its recombinant strains from different carbon sources

Medium	Strain	Ectoine (g/L)	Productivity (mg/L·h)	Conversion efficiency (g/g sugar)
MMG3 (glucose)	J9U	3.06	51.00	0.18
	J9U-P8E	4.24	70.67	0.17
	J9U-P8EC	**5.06**	**84.33**	**0.26**
MMX3 (xylose)	J9U	1.36	22.67	0.06
	J9U-P8E	2.45	40.83	0.11
	J9U-P8EC	**4.12**	**68.67**	**0.21**
MMXG3 (xylose, glucose)	J9U	2.02	33.67	0.07
	J9U-P8E	5.64	94.00	0.20
	J9U-P8EC	**8.55**	**142.50**	**0.32**
MML3 (lignocellulosic hydrolysate)	J9U	0.51	8.50	0.02
	J9U-P8EC	1.30	21.67	0.06

in a 60 h fermentation period and the final CDW of J9U was higher than those of J9U-P8E and J9U-P8EC at 60 h (Fig. 5F and S7). Compared to previous studies using *H. elongata* and *M. alcaliphilum* with the ectoine production of 53.53 mg/g fresh cell weight and 37.93 mg/g CDW [17, 22], 664.52 mg ectoine/g CDW produced by J9U-P8EC is the highest ectoine production obtained using xylose as the sole carbon source so far (Table 2). All ectoine titre and productivity for J9U and its mutant strains can be found in Table 3.

Biosynthesis of ectoine from a glucose-xylose mixture and corn straw hydrolysate

To evaluate the capacity of J9U, J9U-P8E and J9U-P8EC to synthesize ectoine from a glucose-xylose mixture, in this study, the three strains were cultured in MMXG3 for 60 h. The growth trend and sugar consumption rate of the three strains grown in MMXG3 were similar in a 60 h fermentation period (Fig. 4). Notably, the ectoine productivity and sugar conversion efficiency of J9U-P8EC were 142.50 mg/L·h and 0.32 g/g, respectively, with a 3.23- and 3.57-fold increase compared to that of J9U (Fig. 4D). These results highlight the capacity of *H. cupida* J9 to utilize glucose and xylose as the co-carbon sources for ectoine biosynthesis.

Halophilic bacteria can use seawater instead of freshwater as their water source, and their alkaline and high-salt environment eliminates the need for sterilization procedures, thereby reducing the complexity and cost of downstream processing [16]. The use of lignocellulose-rich feedstocks for producing high-value chemicals either fully utilize agricultural waste or reduces the substrate cost of microbial fermentation [19]. In this study, we explored the feasibility of *H. cupida* J9 in synthesizing ectoine from non-sterilized lignocellulosic biomass. Both J9U and J9U-P8EC were cultured in MML3 for 60 h to evaluate ectoine productivity. Both strains exhibited the similar growth rates in an open fermentation process (Fig. 6A). The ectoine productivity and sugar conversion efficiency of J9U-P8EC reached 21.67 mg/L·h and 0.06 g/g, respectively, with a 1.55-fold and 2.00-fold increase compared to that of J9U (Fig. 6B; Table 3). These results highlight the potential of J9U-P8EC to synthesize ectoine from lignocellulosic biomass in an open fermentation system.

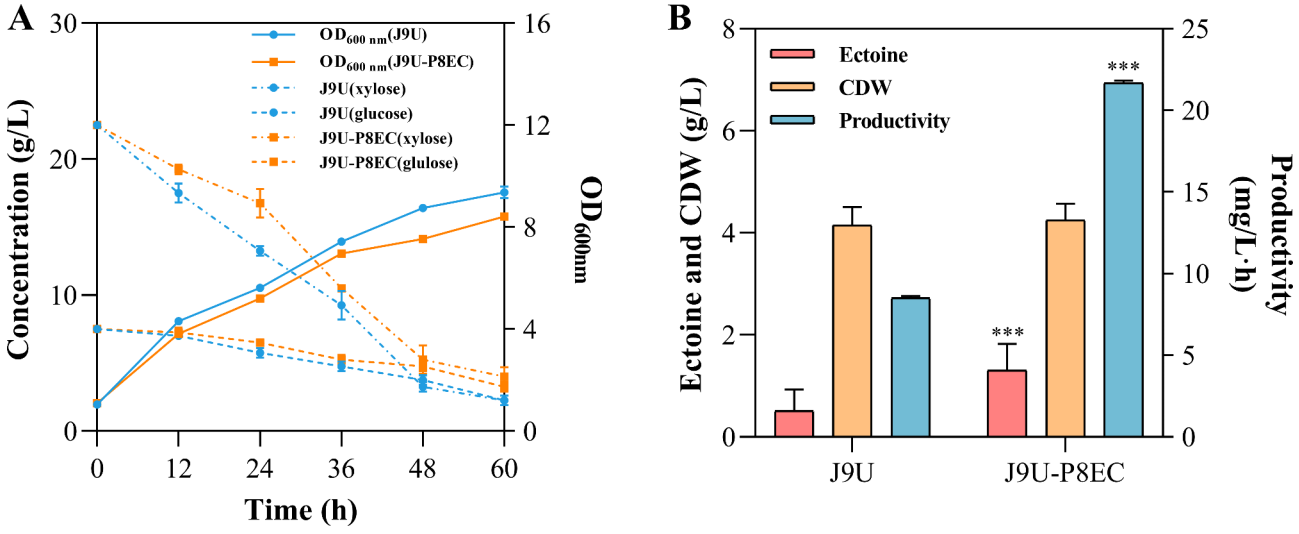

Fig. 6 Cell biomass and ectoine production of MML3-grown J9U and J9U-P8EC. (**A**) Cell growth and total sugar consumption of J9U and J9U-P8EC. (**B**) CDW and the titre and productivity of ectoine obtained by fermentation with J9U and J9U-P8EC. These strains were cultured in MML3 (xylose: glucose = 3: 1, total 30 g/L) at 37 °C and 200 rpm for 60 h in an open fermentation process. The data represent the mean ± standard deviation of triplicate measurements. *** indicates $P < 0.001$

Conclusions

Under salt stress, the transcription levels of ectoine biosynthesis genes are upregulated in *H. cupida* J9 and ectoine accumulation is enhanced. Most ectoine molecules are secreted into the culture medium. The constructed J9U-P8EC has the highest productivity of 142.50 mg/L·h obtained by xylose fermentation so far. Moreover, the capacity of J9U-P8EC to synthesize ectoine from either a glucose-xylose mixture or corn straw hydrolysate highlights the potential of this strain to utilize lignocellulose-rich feedstocks for ectoine production. Utilization of inexpensive substrates by J9U-P8EC for open production of ectoine makes J9U-P8EC an ideal producer for large-scale production of ectoine. In the future, the ectoine yield will be further improved by enhancing the tolerance of J9U-P8EC to inhibitors in lignocellulose hydrolysate and optimizing the fermentation process in a bioreactor.

Supplementary Information

The online version contains supplementary material available at https://doi.org/10.1186/s12934-024-02515-w.

Supplementary Material 1

Supplementary Material 2

Author contributions

YPC, CY and RHL designed this study. YPC, YJL, YM and XTJ performed these experiments. YPC, YJL, YM, XTJ, WNX, SFW, CY and RHL carried out the data analysis. YPC, CY and RHL wrote the manuscript.

Funding

This work was supported by the National Key Research and Development Program of China (2023YFE0104900-4) and the National Natural Science Foundation of China (32101171).

Data availability

No datasets were generated or analysed during the current study.

Declarations

Ethics approval and consent to participate

Not applicable.

Consent for publication

Not applicable.

Competing interests

The authors declare no competing interests.

Received: 22 May 2024 / Accepted: 24 August 2024
Published online: 31 August 2024

References

1. Pastor JM, Salvador M, Argandoña M, Bernal V, Reina-Bueno M, Csonka LN, Iborra JL, Vargas C, Nieto JJ, Cánovas M. Ectoines in cell stress protection: uses and biotechnological production. Biotechnol Adv. 2010;28:782–801.
2. Kunte H-J, Lentzen G, Galinski E. Industrial production of the cell protectant ectoine: protection mechanisms, processes, and products. Curr Pharm Biotechnol. 2014;3:10–25.
3. Kadam P, Khisti M, Ravishankar V, Barvkar V, Dhotre D, Sharma A, Shouche Y, Zinjarde S. Recent advances in production and applications of ectoine, a compatible solute of industrial relevance. Bioresour Technol. 2024;393:130016.
4. Liu M, Liu H, Shi M, Jiang M, Li L, Zheng Y. Microbial production of ectoine and hydroxyectoine as high-value chemicals. Microb Cell Fact. 2021;20:76.
5. Feng Y, Qiu M, Shao L, Jiang Y, Zhang W, Jiang W, Xin F, Jiang M. Strategies for the biological production of ectoine by using different chassis strains. Biotechnol Adv. 2023;70:108306.
6. Goller K, Ofer A, Galinski EA. Construction and characterization of an NaCl-sensitive mutant of *Halomonas elongata* impaired in ectoine biosynthesis. FEMS Microbiol Lett. 1998;161:293–300.
7. Gießelmann G, Dietrich D, Jungmann L, Kohlstedt M, Jeon EJ, Yim SS, Sommer F, Zimmer D, Mühlhaus T, Schroda M, Jeong KJ, Becker J, Wittmann C. Metabolic engineering of *Corynebacterium glutamicum* for high-level ectoine production: design, combinatorial assembly, and implementation

of a transcriptionally balanced heterologous ectoine pathway. Biotechnol J. 2019;14:1800417.
8. Zhao Q, Li S, Lv P, Sun S, Ma C, Xu P, Su H, Yang C. High ectoine production by an engineered *Halomonas hydrothermalis* Y2 in a reduced salinity medium. Microb Cell Fact. 2019;18:184.
9. Ma H, Zhao Y, Huang W, Zhang L, Wu F, Ye J, Chen GQ. Rational flux-tuning of *Halomonas bluephagenesis* for co-production of bioplastic PHB and ectoine. Nat Commun. 2020;11:3313.
10. Jungmann L, Hoffmann SL, Lang C, De Agazio R, Becker J, Kohlstedt M, Wittmann C. High-efficiency production of 5-hydroxyectoine using metabolically engineered *Corynebacterium glutamicum*. Microb Cell Fact. 2022;21:274.
11. Xu S, Zhang B, Chen W, Ye K, Shen J, Liu P, Wu J, Wang H, Chu X. Highly efficient production of ectoine via an optimized combination of precursor metabolic modules in *Escherichia coli* BL21. Bioresour. Technol. 2023;390:129803.
12. Qin Q, Ling C, Zhao Y, Yang T, Yin J, Guo Y, Chen G. Q. CRISPR/Cas9 editing genome of extremophile *Halomonas* spp. Metab Eng. 2018;47:219–29.
13. Xu T, Mitra R, Tan D, Li Z, Zhou C, Chen T, Xie T, Han J. Utilization of gene manipulation system for advancing the biotechnological potential of halophiles: a review. Biotechnol. Adv. 2023;70:108302.
14. Wang S, Liu Y, Guo H, Meng Y, Xiong W, Liu R, Yang C. Establishment of a low-cost polyhydroxyalkanoate production platform from Halomonas cupida J9. Biotechnol Bioeng. 2024;121:2106–20.
15. Fu XZ, Tan D, Aibaidula G, Wu Q, Chen JC, Chen GQ. Development of *Halomonas* TD01 as a host for open production of chemicals. Metab Eng. 2014;23:78–91.
16. Chen G-Q, Jiang X-R. Next generation industrial biotechnology based on extremophilic bacteria. Curr Opin Biotechnol. 2018;50:94–100.
17. Tanimura K, Nakayama H, Tanaka T, Kondo A. Ectoine production from lignocellulosic biomass-derived sugars by engineered *Halomonas elongata*. Bioresour Technol. 2013;142:523–9.
18. Cantera S, Lebrero R, Rodríguez E, García-Encina PA, Muñoz R. Continuous abatement of methane coupled with ectoine production by *Methylomicrobium alcaliphilum* 20Z in stirred tank reactors: a step further towards greenhouse gas biorefineries. J Clean. 2017;152:134–41.
19. Govil T, Wang J, Samanta D, David A, Tripathi A, Rauniyar S, Salem DK, Sani RK. Lignocellulosic feedstock: a review of a sustainable platform for cleaner production of nature's plastics. J Clean. 2020;270:122521.
20. Sohn YJ, Son J, Lim HJ, Lim SH, Park SJ. Valorization of lignocellulosic biomass for polyhydroxyalkanoate production: Status and perspectives. Bioresour Technol. 2022;360:127575.
21. Arhin SG, Cesaro A, Di Capua F, Esposito G. Recent progress and challenges in biotechnological valorization of lignocellulosic materials: towards sustainable biofuels and platform chemicals synthesis. Sci Total Environ. 2023;857:159333.
22. Pham DN, Nguyen AD, Mai DHA, Lee EY. Development of a novel methanotrophic platform to produce ectoine from methane and lignocellulose-derived sugars. Chem Eng J. 2023;463:142361.
23. Saini JK, Saini R, Tewari L. Lignocellulosic agriculture wastes as biomass feedstocks for second-generation bioethanol production: concepts and recent developments. 3 Biotech. 2015;5:337–53.
24. Taha M, Foda M, Shahsavari E, Aburto-Medina A, Adetutu E, Ball A. Commercial feasibility of lignocellulose biodegradation: possibilities and challenges. Curr Opin Biotechnol. 2015;38:190–7.
25. Liu Y, Zhao W, Wang S, Huo K, Chen Y, Guo H, Wang S, Liu R, Yang C. Unsterile production of a polyhydroxyalkanoate copolymer by *Halomonas cupida* J9. Int J Biol Macromol. 2022;223:240–51.
26. Green MR, Sambrook J, Molecular Cloning. A Laboratory Manual. 4th ed. Cold Spring Harbor, NY, USA: Cold Spring Harbor Laboratory Press; 2014.
27. Zhao W, Xiong W, Liu Y, Guo H, Wang S, Chen Y, Liu R, Li B, Yang C. Establishment of a halotolerant bioremediation platform from *Halomonas cupida* using synthetic biology approaches. Chem Eng J. 2023;473:145285.
28. Livak KJ, Schmittgen TD. Analysis of relative gene expression data using real-time quantitative PCR and the 2(−ΔΔC(T)) method. Methods. 2001;25:402–8.
29. Huo K, Liu Y, Huang R, Zhang Y, Liu H, Che Y, Yang C. Development of a novel promoter engineering-based strategy for creating an efficient *para*-nitrophenol mineralizing bacterium. J Hazard Mater. 2022;424:127672.
30. Hou XW, Tong HY, He ZH. Alternative seamless cloning strategies in fusing gene fragments based on overlap-PCR. Mol Biotechnol. 2021;63:221–31.
31. Wang Z, Zhuang J, Wang X, Li Z, Fu Y, Qin M. Limited adsorption selectivity of active carbon toward non-saccharide compounds in lignocellulose hydrolysate. Bioresour Technol. 2016;208:195–9.
32. Orhan F, Ceyran E, Akincioğlu A. Optimization of ectoine production from *Nesterenkonia xinjiangensis* and one-step ectoine purification. Bioresour Technol. 2023;371:128646.
33. Cantera S, Phandanouvong-Lozano V, Pascual C, García-Encina PA, Lebrero R, Hay A, Muñoz R. A systematic comparison of ectoine production from upgraded biogas using *Methylomicrobium alcaliphilum* and a mixed haloalkaliphilic consortium. Waste Manage. 2020;102:773–81.
34. Solomon CM, Collier JL, Berg GM, Glibert PM. Role of urea in microbial metabolism in aquatic systems: a biochemical and molecular review. Aquat Microb Ecol. 2010;59:67–88.
35. Dang Y, Zhao F, Liu X, Fan X, Huang R, Gao W, Wang S, Yang C. Enhanced production of antifungal lipopeptide iturin A by *Bacillus amyloliquefaciens* LL3 through metabolic engineering and culture conditions optimization. Microb Cell Fact. 2019;18:8.
36. Zhang F, Huo K, Song X, Quan Y, Wang S, Zhang Z, Gao W, Yang C. Engineering of a genome-reduced strain *Bacillus amyloliquefaciens* for enhancing surfactin production. Microb Cell Fact. 2020;19:223.
37. Zhang Y, Liu H, Liu Y, Huo K, Wang S, Liu R, Yang C. A promoter engineering-based strategy enhances polyhydroxyalkanoate production in *Pseudomonas putida* KT2440. Int J Biol Macromol. 2021;191:608–17.
38. Tan B, Zheng Y, Yan H, Liu Y, Li Z-J. Metabolic engineering of *Halomonas bluephagenesis* to metabolize xylose for poly-3-hydroxybutyrate production. Biochem Eng J. 2022;187:108623.
39. Liu H, Chen Y, Wang S, Liu Y, Zhao W, Huo K, Guo H, Xiong W, Wang S, Yang C, Liu R. Metabolic engineering of genome-streamlined strain *Pseudomonas putida* KTU-U27 for medium-chain-length polyhydroxyalkanoate production from xylose and cellobiose. Int J Biol Macromol. 2023;253:126732.
40. Schäfer A, Tauch A, Jäger W, Kalinowski J, Thierbach G, Pühler A. Small mobilizable multi-purpose cloning vectors derived from the *Escherichia coli* plasmids pK18 and pK19: selection of defined deletions in the chromosome of *Corynebacterium glutamicum*. Gene. 1994;145:69–73.

Publisher's note